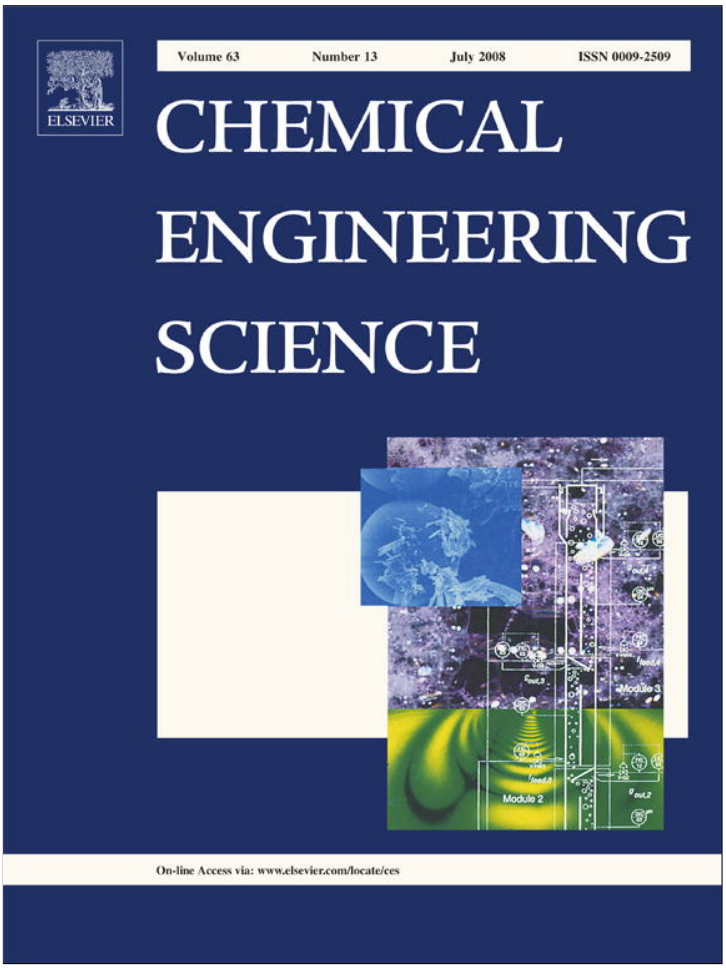

Chemical Engineering Science 63 (2008) 3438 – 3448

Contents lists available at ScienceDirect

Chemical Engineering Science

journal homepage: www.elsevier.com/locate/ces

Nucleation, growth and detachment of neighboring bubbles over miniature heaters

Thodoris D. Karapantsios[a,*], Margaritis Kostoglou[a], Nikolaos Divinis[a,b], Vasilis Bontozoglou[b]

[a]Department of Chemistry, Division of Chemical Technology, Aristotle University, University Box 116, 541 24 Thessaloniki, Greece
[b]Department of Mechanical Engineering, University of Thessaly, Pedion Areos, 38 334 Volos, Greece

ARTICLE INFO

Article history:
Received 20 July 2007
Received in revised form 5 March 2008
Accepted 3 April 2008
Available online 6 April 2008

Keywords:
Bubble growth
Degassing
Bubble nucleation
Bubble detachment
Low gravity

ABSTRACT

This work investigates how simultaneous CO_2 bubbles desorb from water and *n*-heptane when these liquids become supersaturated with dissolved CO_2. Supersaturation is imposed locally by a miniature heater so bubbles grow at adjacent sites across the heater. To suppress buoyancy, experiments are performed at low gravity conditions. The number of nucleation sites and nucleation time delay depend on liquid properties and heating power. Simultaneous bubbles do not grow at exactly the same rate and calculations show that this corresponds to slightly different bubble temperatures. Moreover, they exhibit smaller growth rates than single bubbles at similar conditions, an indication that they compete for dissolved CO_2. As bubbles expand into the surrounding cold liquid, the heater's temperature decreases in a fashion implying the inception of Marangoni convection. Simultaneous bubbles detach due to g-jitters but following different ways in the two liquids. However, they always detach together and at smaller sizes than single bubbles do. A temperature triggered destabilization of contact lines is deemed responsible for this.

1. Introduction

The study of bubble nucleation, growth and detachment during the desorption of dissolved gases (degassing) in liquids is significant for the effective design of many industrial equipment. In many applications degassing is caused by a reduction of the system pressure at ambient temperature, e.g. in cavitating turbines and pumps (Payvar, 1987), in carbonated drinks (Barker et al., 2002) and in liquid waste treatment by dissolved air flotation (Malley and Edzwald, 1991). In another class of applications desorption of dissolved gases is caused by rising the system temperature, e.g. in the degassing of glass melts and glass powders (Heide et al., 1996; Yamasaki et al., 2007), in the degassing of alloy powders (Nyborg and Magalhuaes, 1996) and in the degassing of metal–carbon selective surfaces (Harding and Window, 1982). Moreover, in many thermal processes, e.g. heat exchangers, boilers, distillation columns, spray dryers etc., degassing of liquid layers during heating has a detrimental side effect which reduces not only the liquid heat transfer coefficients but also the evaporation rates by forming layers of air that spread over hot surfaces (McCabe and Smith, 1967; Kern, 1950). While decompression degassing has a global volume effect, thermal degassing is usually imposed locally by hot vessel walls or submerged heaters and so it inevitably yields temperature gradients (non-isothermal conditions) across the liquid volume. Using partial vacuum to enhance degassing lowers but does not extinct temperature gradients (Kern, 1950; Szekely and Fang, 1973).

Early studies on bubble dynamics were performed having in mind vapor bubbles controlled by heat transfer (nucleate boiling) rather than dissolved gas bubbles where mass transfer dominates (desorption). Several of those pioneering studies focused on the spherically symmetric growth of *single*, isolated, bubbles controlled by heat transfer inside infinite liquids of constant superheat (Plesset and Zwick, 1954; Forster and Zuber, 1954). Among the few reported analytical solutions, the simple parabolic law ($R \sim t^{\alpha=0.5}$, where R the bubble radius and t the time of growth) introduced by Scriven (1959) has been particularly successful in describing single bubble growth in uniform temperature fields, i.e., during nucleate boiling. The same expression proved also useful in describing the isothermal mass-diffusion induced bubble growth from supersaturated (with dissolved gas) solutions (Barker et al., 2002; Glas and Westwater, 1964; Bisperink and Prins, 1994; Jones et al., 1999a,b).

Recent experimental and theoretical works from this group (Divinis et al., 2004, 2005, 2006a,b; Kostoglou and Karapantsios, 2005, 2007) on the dynamics of liquid degassing showed that single bubbles growing over submerged heaters (thus within temperature gradients) deviate from the parabolic law to an extent depending on the liquids physical properties which dictate the growth rate; the slowest the growth rate the nearest to $\alpha = 0.5$.

Regarding the production of *multiple* simultaneous bubbles during the desorption of dissolved gases, Scriven's solution was tested

* Corresponding author. Tel.: +30 2310 99 7772; fax: +30 2310 99 7759.
E-mail address: karapant@chem.auth.gr (T.D. Karapantsios).

0009-2509/$ - see front matter © 2008 Published by Elsevier Ltd.
doi:10.1016/j.ces.2008.04.002

by Westerheide and Westwater (1961) in (isothermal) electrolysis experiments. These authors found that bubbles produced by coalescence of smaller neighboring bubbles do not follow the parabolic growth law but in that case $\alpha \approx 0.3$. Irregular bubble growth under isothermal conditions was also observed by Buehl and Westwater (1966) when producing multiple carbon dioxide bubbles on a solid substrate by decompression of liquids at high levels of supersaturation. The divergence from the parabolic law was again attributed to coalescence of bubbles from neighboring sites. The above studies demonstrated that multiple bubbles even under isothermal conditions do not grow according to the ideal parabolic law.

The heterogeneous nucleation of boiling (vapor) bubbles on solid walls is an evergreen field of research. Boiling experiments have shown that the nucleation time delay depends on the local heat flux and the interfacial and hydrodynamic conditions at the cavity (Merte and Lee, 1997; Lee et al., 2003; Li and Peterson, 2005). Kant and Weber (1994) in order to study the stability of nucleation sites in pool boiling, observed the penetration of liquid in heated glass capillaries following bubble detachment. They noticed that the depth of penetration of the liquid/gas interface was influenced by the surface tension, the viscosity and the wetting ability of the liquid as well as by the geometry of the capillary.

In studies of heterogeneous nucleation during degassing of liquids, bubbles of a dissolved gas were customarily produced by a homogeneous decompression or a global increase in the temperature of a liquid (Jones et al., 1999a,b; Liger-Belair et al., 2002, 2005). Buehl and Westwater (1966) and recently, Jones et al. (1998) noticed that in cases where several bubbles were produced sequentially at a specific nucleation site, every next bubble had a longer nucleation delay time than its predecessor, indicating a localized solute depletion at the region of the nucleation site. Liger-Belair et al. (2002) attributed this progressively lower bubble production rate to the depletion of $CaCO_3$ nuclei at the vessel walls (initially deposited there during washing with tap water). Trying to test existing theoretical relations for estimating bubble hetero-nucleation rates Lubetkin (1989a,b) used an acoustic technique to count the number of bubbles produced during nucleation in carbonated water in order to identify a correlation between number of bubbles and nucleation rate. Later, Lubetkin (1995) recognized the existence of a relationship between nucleation time delay rate and initial bubble growth. Nevertheless, more work is required to investigate the parameters that affect nucleation from cavities during degassing and how this is related to subsequent bubble growth.

Bubble departure is an important parameter determining the amount of gas production at a surface. As bubbles depart, a portion of their gas remains in the sites providing nuclei for the formation of new bubbles (Kant and Weber, 1994; Liger-Belair et al., 2002, 2005). The size and frequency of bubbles ejecting from a surface affect the temperature and concentration boundary layers over the surface since bubbles are replaced by fresh liquid from the bulk. Interestingly, bubbles depart from the surface at much smaller sizes than predicted by a simple force balance analysis. To account for this, Mori (1998) proposed a surface tension aided mechanism for bubble departure which is caused by the formation and collapse of the bubble neck. This is opposite to existing theories which claim that surface tension acts to retain the bubbles at the wall. Under low gravity conditions individual bubbles remain attached to the heater surface for longer times and therefore grow up to excessively large sizes. Straub et al. (1990, 1992) observed that bubbles at microgravity remain about 10 times longer at the heater surface and grow to a diameter 3–4 times larger than in 1-g before their departure (mainly due to g-jitters). Cooper et al. (1978) based on their microgravity experiments also concluded that the effect of surface tension was to assist the departure of bubbles.

The scope of the present work is to study the dynamics of multiple neighboring bubbles forming during the desorption of carbon dioxide from supersaturated water and *n*-heptane. A small axisymmetrical thermistor is used as a heater in order to create local supersaturation (superheating) in a large pool of cold saturated solution. Experiments are performed below the boiling point of the liquid but yet at quite elevated temperatures where vapor pressure is significant. This work is an extension of our previous work on single bubbles growing over submerged heaters. Multiple bubbles growing over flat plate heaters were also dealt with (Divinis et al., 2006b). The present experiments are conducted at low gravity conditions in order to: (1) suppress natural convection of liquid thermal layers around the heater, (2) minimize buoyancy bubble distortion and (3) allow bubbles to grow up to large sizes without departing from the heater. To our knowledge, these are the first experiments of diffusion-induced multiple bubble production of a dissolved gas that are performed in weightlessness.

The outline of the work is as follows: First, a summary of a recent model developed for spherically symmetric non-isothermal bubble growth is presented. Next, the experimental setup used in two ESA's (European Space Agency) parabolic flight campaigns is presented briefly. The primary experimental information involves data of the evolution of bubble radius and heater temperature for water and *n*-heptane and for various heating powers. Finally, the experimental results are compared with theoretical predictions and against results of single bubble growth in order to interpret the observed phenomena.

2. Theory

A detailed mathematical description of the process of a bubble growing while attached to a heated wall includes the solution of transient heat and mass transfer equations in the gas and liquid phases along with the appropriate boundary conditions on the surface of the bubble and the heater. These equations are of the convection–diffusion type where the flow field responsible for the convection terms is generated by the expanding bubble. Evidently, the problem includes moving boundaries with the motion being part of the solution. In addition, the temperature gradient along the surface of the bubble induces a Marangoni motion which transfers hot fluid from the heater to the remote parts of the bubble surface, tending to equilibrate the bubble and the heater temperatures. The presence of multiple bubbles growing in proximity complicates further the process because of the interaction between the flow, temperature and concentration fields around these neighboring bubbles.

Although the complete problem can in principle be formulated, its numerical solution is very difficult. Problems like the inherent three dimensionality, the moving gas–liquid interface and the inclusion of Marangoni effects could be technically handled using advanced CFD codes employing the so-called volume of fluid (VOF) technique to track the interface evolution. Yet, the stiffness of the problem under the specific experimental conditions is so large (initially explosive bubble growth, extremely large Marangoni number) that precludes the possibility of numerical solution at reasonable computation times. Only very recently, the Marangoni flow around *non-growing* bubbles in a similar situation (stationary or moving bubbles attached to a thin heated wire) has been addressed by Christopher et al. (2006).

Our first attempt to simulate the problem was based on a spherically symmetric (1-D) model for the liquid around a bubble which grows at a uniform and constant (time independent) temperature (Divinis et al., 2004). The problem was solved using a well-known similarity transformation that has led to a power law relation between bubble radius and time with an exponent value equal to 0.5 which gave predictions close to the measured data for short bubble growth times (up to 1–2 s). For larger times, the experimental curves were best-fitted by lower (than 0.5) exponent values which

essentially meant that the bubble temperature was decreasing with time. The possibility that the discrepancy was due to the temperature dependent physical properties of the surrounding liquid or a radial temperature distribution inside the bubble was dealt with in a previous publication (Divinis et al., 2005) which showed that those factors could not explain the discrepancy.

Keeping in mind that the driving force for bubble growth is the difference between the dissolved gas bulk concentration and the equilibrium concentration (solubility) at the bubble surface, one can go a step further. The problem can be approximated by a 1-D model for the liquid assuming that the bubble grows under a time dependent temperature. This temperature represents the spatially average temperature across the whole bubble at every instant. It must be noted that the volumetric and surface average temperatures of the bubble coincide, since the intra-bubble temperature field is dictated by pseudo-steady state heat conduction (Laplace) equation.

It is apparent that the computation of the evolution of the instantaneous average bubble temperature requires knowledge of the complete temperature field which is not known. So, based on the simplified 1-D model, the inverse problem can be formulated. This calls for estimating the average bubble temperature evolution curve, $T_b(t)$, from the experimental bubble growth curve, $R(t)$. Comparing the estimated evolution of the average bubble temperature with the measured evolution of the heater temperature reveals important information on the phenomena governing bubble growth. It must be stressed that the inverse problem does not involve the energy balance on the bubble surface (including terms such as latent heat, heat capacity of gas/vapor, heat of gas dissolution, gas expansion work etc.) since the bubble temperature is exclusively deduced from heat and mass transfer considerations on the liquid side combined with the bubble growth curve. Details of this approach can be found in Divinis et al. (2006a).

The outcome of the inverse 1-D mathematical problem is that at every instant the average bubble temperature $T_b(t)$ can be estimated from the experimental bubble radius evolution curve through the following transcendental equation:

$$\left(\left[2F_m D\left(\frac{T_o+T_b}{2}\right)\right]^{-0.8}+\left[\frac{12}{\pi}F_m^2 D(T_b)\right]^{-0.8}\right)^{-1.25} = \left(\frac{\mathrm{d}R^2}{\mathrm{d}t}\right)_{\mathrm{exp}} \quad (1)$$

where $D(T)$ is the temperature dependent gas-in-liquid diffusion coefficient and T_o is the far field bulk temperature. The foaming number F_m is defined as

$$F_m = \frac{(c_{\mathrm{sat}}(T_o)-c_{\mathrm{sat}}(T_b))R_g T_b}{P_\infty - P_{\mathrm{sat}}(T_b)} \quad (2)$$

where c_{sat} is the solubility of the gas in the liquid, P_{sat} the vapor pressure of the liquid, P_∞ the ambient pressure and R_g the ideal gas constant. This number denotes the ratio of the relative contributions of convection over diffusion transport of CO_2 from the bulk to the bubble surface.

3. Experiment

The experimental setup has been described elsewhere in detail (Divinis et al., 2004, 2006a). Here the major components are presented briefly.

The core of the equipment is an ultra precision thermostat unit into which an exchangeable sample cell unit is inserted (Fig. 1). The thermostat operates under the gradient reduction principle and can provide temperature stability in the order of ±0.005 °C. A sample cell unit is essentially a sealed tube the lower part of which is made of special spectrometer glass cuvette. The cells are specially designed

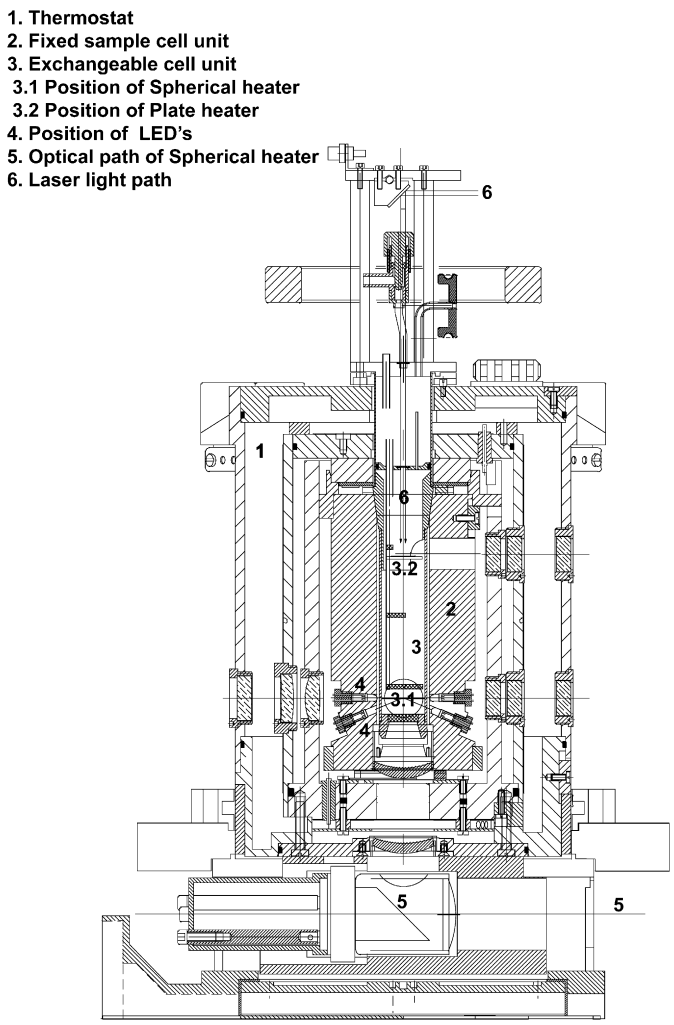

Fig. 1. Engineering drawing of the thermostat unit with an exchangeable cell.

to maintain their measuring chamber (glass cuvette) completely full with liquid at all times so as to prevent free float of the liquid in low gravity. The liquid volume in the cell is approx. 22 cm^3. The pressure inside the cells is kept at ambient values by means of an elastic membrane sealing a port of the cell. This work presents only results of multiple bubbles growing adjacent to each other on the glass-coated surface of a small, roughly spherical, NTC thermistor (Thermometrics, Inc. $r_{\mathrm{th}} = 0.125$ mm, nominal) serving as a local heater. In fact, the thermistor is an axisymmetric ellipsoid with a small-to-large radii ratio of 1:2; the value of the nominal radius represents the two small, approximately equal, radii. It must be stressed that the recording view of the thermistor provides a roughly spherical 2-D projection in the plane of the two smaller radii.

The bubbles growing on the spherical heater are illuminated by three sets of RGB light emitting diodes (LEDs) located apart by 120° around the circumference of the cell. The illumination coming from one of these sets is offset by 7° in the longitudinal direction in order to allow a 3-D impression on the 2-D images. To enhance the contrast between the bubble and its surroundings a 5 mW He–Ne laser is used for background illumination. Bubble images are recorded by a CCD color camera with 1 k × 1 k pixels, 24-bit resolution RGB and acquisition rate of 25 frames per second. An image processing code written in MATLAB® is used to determine the bubble diameter versus time from video frames. The overall uncertainty in the determination of bubble radius is ±2%.

Table 1
Range of the delivered powers and the heater temperatures which produced multiple bubbles in both test liquids

Liquid	Power range (mW)	Heat flux range (W/m^2)	$T_{ave.}$ range[a] (°C)
Water	46.0–66.0	5.6×10^4–8.0×10^4	83.0–91.0
n-heptane	13.0–86.0	1.6×10^4–1.0×10^5	42.0–89.0

[a]T_{ave} temperature calculated from data through the entire heating runs.

Bubbles are produced at the surface of the thermistor by applying continuous heat pulses of constant power (±2%). The power of the pulses is constant through each run but varies among runs. The duration of each heat pulse is either 10 or 20 s. Registering the voltage drop across the thermistor allows the delivered power and temperature of the thermistor to be estimated. Table 1 displays the range of the delivered power levels for the different test liquids which produced multiple bubbles. The corresponding ranges of the average thermistor temperatures and estimated heat fluxes—assuming that the heater is perfectly spherical—are also presented.

De-ionized water and *n*-heptane (99.0%, Panreac quimica) are the test liquids in this work. These liquids are initially saturated by prolonged bubbling with CO_2 (99.99%, Air metal).

The experiments are conducted during the 35th and 38th ESA's Parabolic Flight Campaigns. Each run is conducted during a separate parabola. Data of onboard gravitational acceleration provided by ESA showed only a moderate quality of low gravity with random fluctuations $\pm 2.6 \times 10^{-2} g$. The low gravity period is slightly different among parabolas but on the average lasts approx. 20 s.

4. Results and discussion

4.1. Thermal data

Fig. 2 displays the applied heating powers versus the ensuing heating thermistor temperatures for generating single and multiple bubbles in water and *n*-heptane, respectively. Temperatures are average values over the entire duration of heating runs. For *n*-heptane, data for two different heating thermistors (test cells) are shown.

Higher power levels (thus temperatures) are necessary to generate bubbles in water than in *n*-heptane chiefly because of the much lower solubility of carbon dioxide in water (Perry and Chilton, 1973; Fogg and Gerrard, 1991). Also, higher power levels are needed to produce multiple bubbles compared with those used to create single bubbles. Yet, these power levels vary among heating thermistors since their nucleation sites demand different thermal energy to be activated. For each thermistor and test liquid a roughly linear relation is noticed between applied power and thermistor temperature, highlighting the strong association between these two parameters.

4.2. Bubble growth generations

For low power heat pulses, Divinis et al. (2004, 2006a) observed single bubbles growing always at the same location of the thermistor surface for the entire heating period. At the higher power levels of this work, two or more bubbles are noticed to grow simultaneously at different (but always the same) locations on the thermistor's surface.

A typical sequence of events during the present heating runs is as follows: after energizing the heater, a brief time lap (depending on the liquid and the applied power) is necessary to create local supersaturation and therefore cause nucleation. Then, a first bubble forms at a specific site on the thermistor and begins to grow. Either simultaneously or with some time delay (depending also on the liquid and the applied power), a second bubble emerges at another nucleation site on the thermistor surface. At some point in time (within the heating period), the on-growing bubbles depart from the heater

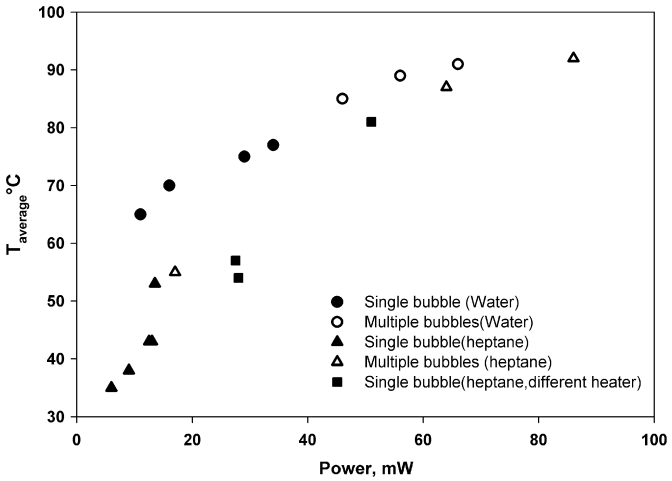

Fig. 2. Applied heating powers and attained average thermistor temperatures for producing multiple and single bubbles in water and in *n*-heptane.

synchronously. This series of events will be henceforth referred to as the 1st *bubble generation* of the heating run. Almost immediately after departure, two new bubbles appear at exactly the same nucleation sites and start growing until they also eventually detach from the heater. This series of events designates the 2nd *bubble generation*. The sequence of bubble generations continues until the end of the heating run or until the end of the low gravity period, whichever comes first. Deviations from the above description are encountered with the highest power pulses employed in *n*-heptane, where bubble generations consist of more than two simultaneous bubbles and detachment is more complicated (see below).

In the plots that follow the [x_x_x, x] format in the legend stands for [day_parabola_campaign, power]. Each plot includes bubble radius evolution curves, the corresponding thermistor (heater) temperature profiles and a sketch with three circles. The circle with the mesh in the middle represents the thermistor, whereas the black and white circles designate the specific locations (nucleation sites) where the two bubbles grow. Accordingly, these two bubbles are described by the black and white markers in the growth curves, respectively. The presented curves correspond only to data obtained during low gravity conditions although heat pulses may last longer. At the top of each plot, *G* denotes the order of bubble generation and *b* the number of bubbles in each generation.

Fig. 3 displays bubble growth data and thermistor temperatures for runs in water. In these experiments, there are always two bubbles per generation. The inability to apply higher powers in water (due to technical reasons) did not permit production of more than two simultaneous bubbles. A general observation is that the two bubbles do not grow at *exactly* the same rate but, usually, bubbles produced on the 1st site (black markers) grow a bit faster than those on the 2nd site (white markers) at least for a part of the growth period. This is perhaps not so clear in some bubble generations at the higher power runs of Figs. 3b and c where the two bubbles appear during some periods to grow at comparable rates (yet, there are differences as explained in Fig. 5a). A tentative explanation for the above is provided below based on the estimated average bubble temperatures.

On the other hand, the growth curves of simultaneous bubbles from successive generations that develop at the same nucleation site usually coincide (within experimental noise) if superimposed. This was also noticed with single bubble generations growing in *n*-heptane (Divinis et al., 2004) and agrees with observations made in earlier mass diffusion-induced bubble growth experiments (Jones et al., 1999b; Westerheide and Westwater, 1961). Inspection of the

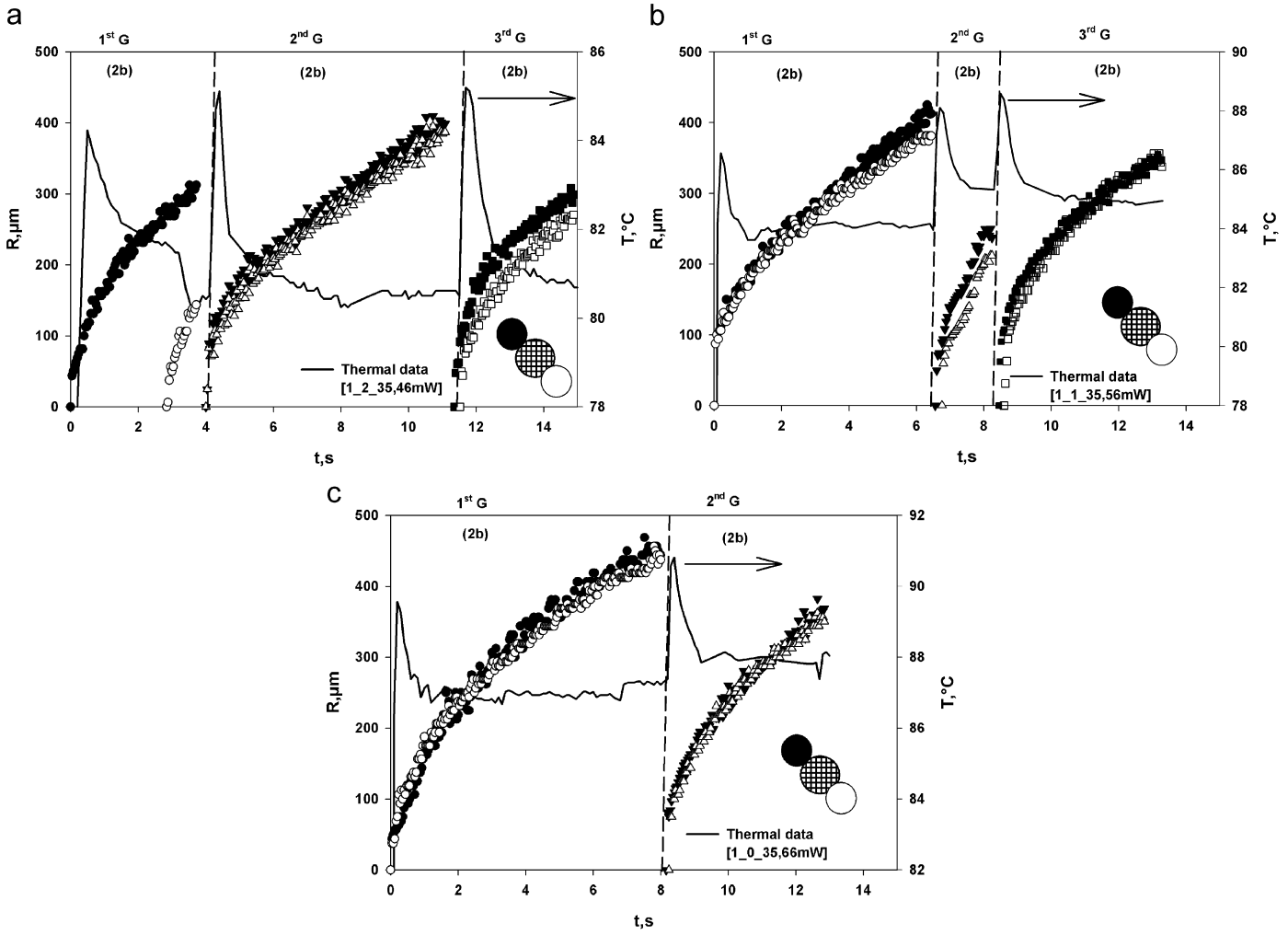

Fig. 3. Multiple bubble growth and heating thermistor temperature data for water. (a) 46 mW, (b) 56 mW, (c) 66 mW.

growth curves of single and double bubbles in Fig. 3a shows that the growth rate is related to the instantaneous heater temperature (thus, to the bubble temperature). Therefore, at the first second of growth, the double bubbles of the 2nd and 3rd generations grow faster than the single bubbles of the 1st generation since the heater is hotter in the 2nd and 3rd generations but this gradually fades out since the heater temperature drops faster during the double bubble growth.

At first glance, it seems strange in Fig. 3c that the number of generations drops from three to two when using a higher power (66 mW) while the opposite would be intuitively expected. It is believed that this is simply because the 66 mW run was the first one conducted with this heating thermistor (test cell) and so its nucleation sites were not activated before.

The temperature of the thermistor follows a pattern related to the bubble production sequence described above. Initially (just before nucleation) the temperature rises very fast because of the thermistor's low heat capacity. After a bubble appears, the thermal behavior of the thermistor is affected by the instantaneous size of the developing bubble relative to the size of the thermistor. So, when the bubble is much smaller than the thermistor, the thermistor temperature continues to climb fast (perhaps not as fast as before nucleation but there is not enough time resolution in temperature readings to assert this). When the bubble reaches a critical size (roughly equal to half the size of the thermistor), the temperature attains a peak value after which it falls—rapidly first, more gradually later—toward a roughly constant value. The latter constant value occurs when the bubble reaches approximately twice the size of the thermistor. Finally, at bubble detachment the temperature rises steeply again and the cycle is repeated. It must be stressed here that in some few runs where accidentally no bubble appeared on the thermistor during heating, the measured thermistor temperature was monotonously increasing with time.

The above sequence is similar to what was observed in single bubble experiments regarding either degassing (Divinis et al., 2004) or boiling (Lee et al., 2003). Yet, the presence of simultaneous growing bubbles affects the thermal behavior of the thermistor. Thus, with just one bubble the decline of the thermistor temperature after its peak value is less steep (e.g. 1st generation in Fig. 3a) than with two simultaneous bubbles (e.g. 2nd and 3rd generations in Fig. 3a). Furthermore, the moment a second bubble forms the temperature immediately drops further. Regarding bubble detachment, similar temperature spikes have been observed to accompany bubble departure from the heater in nucleate boiling experiments (Chen and Chung, 2002) as the insulating effect of bubbles over the heater was momentarily eliminated.

The aforementioned characteristic variation of the thermistor temperature may be qualitatively interpreted by considering the development of Marangoni convection around the bubble which drives liquid away from the hot and toward the cold side of the gas/liquid interface. In this way, the bubble acts as a microscale pump dragging

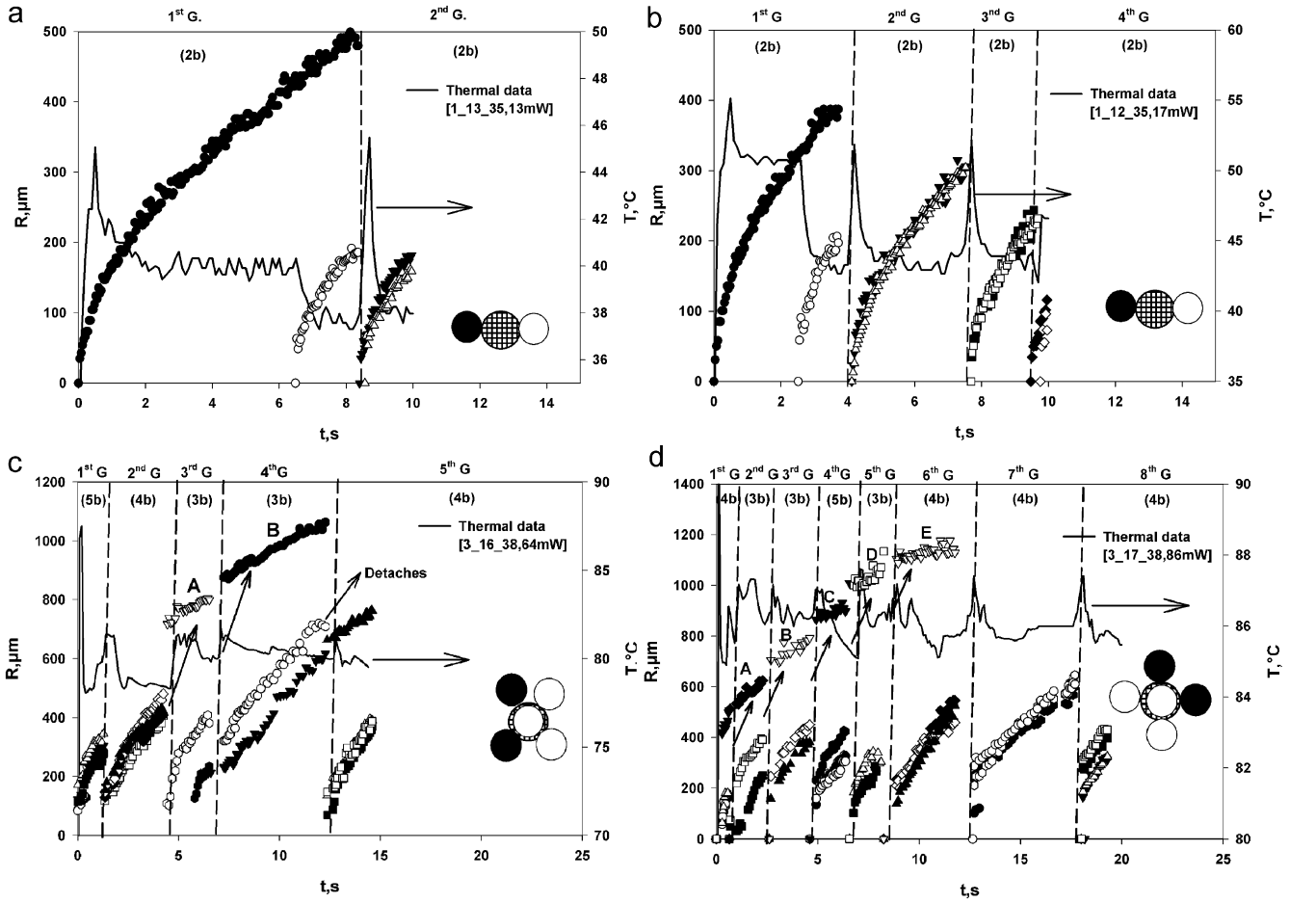

Fig. 4. Multiple bubble growth and heating thermistor temperature data for *n*-heptane. (a) 13 mW, (b) 17 mW, (c) 64 mW, (d) 86 mW.

liquid from the region adjacent to the thermistor surface toward the bulk. Such Marangoni convection has been repeatedly reported in subcooled boiling applications (Christopher et al., 2006; Petrovic et al., 2004).

The instantaneous thermistor temperature reflects the synchronous contribution of two effects: (1) an electric heating effect which tends to increase the temperature and (2) Marangoni convection around the bubble which tends to reduce the temperature. While the intensity of electric heating is constant, the intensity of Marangoni convection depends on the overall temperature difference between the hot and cold end of the bubble, thus, it varies with bubble size. The data show that as soon as the growing bubble reaches about half the size of the thermistor the thermistor begins to cool down, a sign that at this point Marangoni convection may start to dominate over electric heating. Eventually, when the bubble becomes large enough for its cold end to attain the temperature of the bulk, Marangoni convection reaches a maximum steady state. The above maximum limit is considered responsible for the establishment of a roughly constant minimum thermistor temperature at the later (and prolonged) stages of bubble growth.

The thermistor profile from one bubble generation to the next drifts slightly toward higher values. The above behavior is attributed to the progressively higher liquid temperatures established around the thermistor after each bubble detachment, as compared to the low bulk temperature before the first heat pulse. This behavior quantitatively varies among heating thermistors as one can see by comparison with the data of Divinis et al. (2004).

Figs. 4a–d display multiple bubble growth runs in *n*-heptane and indicate a dramatic increase in complexity with power level. For the lower employed powers (13 and 17 mW; Figs. 4a and b) observations are alike to water. The evolution of the thermistor temperature from the 1st bubble generation to the next appears now to overall drift toward lower values but this is simply because the creation of the second bubble in the 1st generation reduces the temperature significantly. In addition, the growth rates of the two simultaneous bubbles differ now less than in water (more about this in the next section). Comparison between the growth curve of the single (1st generation) bubble in Figs. 4a and b and the successive double bubbles at the same site reveals that single bubbles grow a bit faster than double bubbles. As with water, this may be partially attributed to all along the higher thermistor temperature during single bubble growth.

The situation is more complex in Figs. 4c and d where due to the very fast growth of several (more than two) simultaneous bubbles, the bubble evolution curves and the thermistor temperature profiles are disturbed. The capital letters (A–E) in Figs. 4c and d denote bubbles (still in contact with the thermistor) that are produced from the coalescence of earlier smaller bubbles. This event will be discussed below with respect to its relevance to bubble departure.

For *n*-heptane, one can see that the number of bubble generations increases as the delivered power increases. Furthermore, at higher power levels the number of bubbles per generation increases, too. This manifests the direct dependence of the number of active nucleation sites on power level, a feature well known in boiling literature (Mori, 1998).

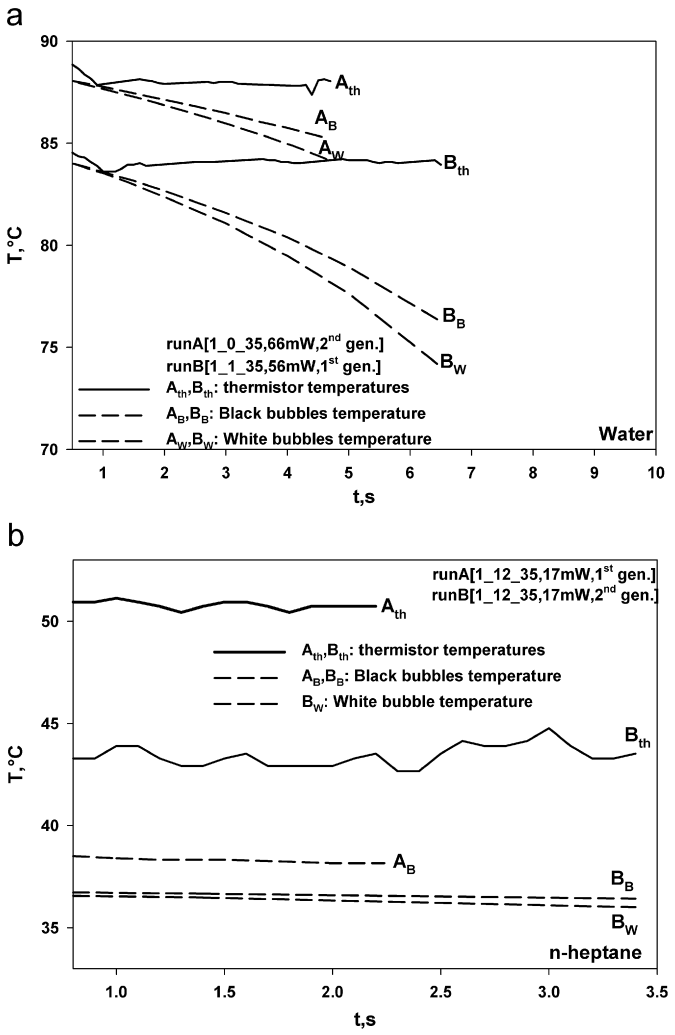

Fig. 5. Average bubble temperature computed from the model compared with measured thermistor temperature for (a) water, (b) *n*-heptane.

4.3. Bubbles temperature versus heater temperature

The non-isothermal model described above predicts the temporal evolution of the spatially average bubble temperature from the experimentally measured radius evolution data. Such predictions are compared with measured thermistor temperatures in Fig. 5. Curves A_{th} and B_{th} correspond to the experimentally obtained thermistor temperatures of runs A and B, respectively. Symbols A_B, B_B and A_W, B_W denote the predicted temperatures corresponding to bubbles with black markers and white markers, respectively.

Two cases of dual-bubble growth are examined for water: one at high power (A; 66 mW) and one at low power (B; 56 mW), Fig. 5a. In both runs, the model predicts that the bubbles temperatures are comparable $\pm 0.05\,^{\circ}C$) to the heater's temperature and to each other for times less than ~ 0.5 s. This prediction is consistent with previous results in water where single bubbles were triggered by lower powers (Divinis et al., 2006a). Since higher powers are necessary to produce multiple bubbles, the duration of isothermal growth is less than in single bubble runs.

It was noted for water (Fig. 3) that bubbles growing on the 1st site (black markers) usually grow faster than those on the 2nd (white markers). This is verified by the model predictions in Fig. 5, which show that the black-marked bubbles attain gradually higher temperatures that the white-marked bubbles. A tentative explanation for the above site-specific bubble growth is that, since the thermistor is not perfectly spherical the thermal boundary layer surrounding it, is also not perfectly symmetrical. Thus, bubbles growing on the 2nd site may correspond to higher-curvature regions of the boundary layer and so extend faster into the colder bulk liquid than bubbles on the 1st site. The possibility that differences in the geometry of the two nucleation cavities might dictate this divergence should rather be excluded due to the slow diffusion-induced growth of large gas bubbles although it is in principle possible such differences to play a key role in the much faster vapor bubbles during boiling.

Fig. 5b compares predicted bubble temperatures to measured thermistor temperatures, for runs in *n*-heptane. Run A refers to growth of a single bubble during the 1st generation (i.e. before activation of the 2nd site). Run B refers to the 2nd generation of the same experiment, where two bubbles grow simultaneously. A strong deviation between heater temperature and bubbles temperatures ($\sim 13\,^{\circ}C$ for run A and $\sim 7\,^{\circ}C$ for run B) is observed very early in both runs. In addition, the two different bubbles temperatures in run B diverge only slightly between each other, in line with the observations made in Fig. 4b.

For single bubbles in *n*-heptane Divinis et al. (2006a) found that for slow growth rates, i.e. low power levels, bubbles were in thermal equilibrium with the thermistor during the entire heating course. On the contrary, at higher power levels strong deviations between thermistor and bubble temperature were observed already after the onset of heating. This was attributed to the much faster bubble expansion rates into the surrounding cold liquid layers encountered at high powers.

Interestingly, in those of the present tests where two simultaneous bubbles occur, the observed growth rates are comparable between water and *n*-heptane although they are triggered by different heating powers and despite the different temperature of bubbles in the two liquids (Figs. 5a and b). In an effort to explain the situation, one might look for probably different Marangoni effects in the two liquids. However, in both liquids the Marangoni number is extremely large so no major differences are expected due to thermocapillarity variations. In addition, one might also think of probably different pre-nucleation temperature profiles around the thermistors (into which then the bubbles develop). However, differences in the nucleation time delay between the two liquids are too small to be responsible for this. Therefore, another explanation must be sought. Although the amount of dissolved gas is higher in *n*-heptane than in water, the progression of heat in *n*-heptane is much slower than in water because the thermal diffusivity of *n*-heptane is two times lower than of water and also because of the lower temperatures employed in *n*-heptane. As a consequence, a bubble growing in *n*-heptane comes sooner in contact with surrounding cold liquid layers than in water. At present this appears the most probable explanation for the similar growth rates in the two liquids.

4.4. Single bubble versus multiple bubble growth rates

Fig. 6a (water) and Fig. 6b (*n*-heptane) compare single bubble against multiple bubble growth data. In the legend of the plots, the average (over the entire heating period) thermistor temperature is shown after the power value. It is observed that the growth curves are alike, in spite of the difference in the average thermistor temperatures in each experimental pair ($5.4\,^{\circ}C$ for water and $3.1\,^{\circ}C$ for *n*-heptane, respectively). The smaller growth rate of the simultaneous bubbles (despite the higher thermistor temperature triggering it) may be attributed to the bubbles competition for carbon dioxide dissolved in the neighborhood of the thermistor. The same argument has been invoked by Westerheide and Westwater (1961) in their electrolysis experiments. Further to this, a closer inspection of Figs. 6a and b shows that at very short times when the two bubbles are

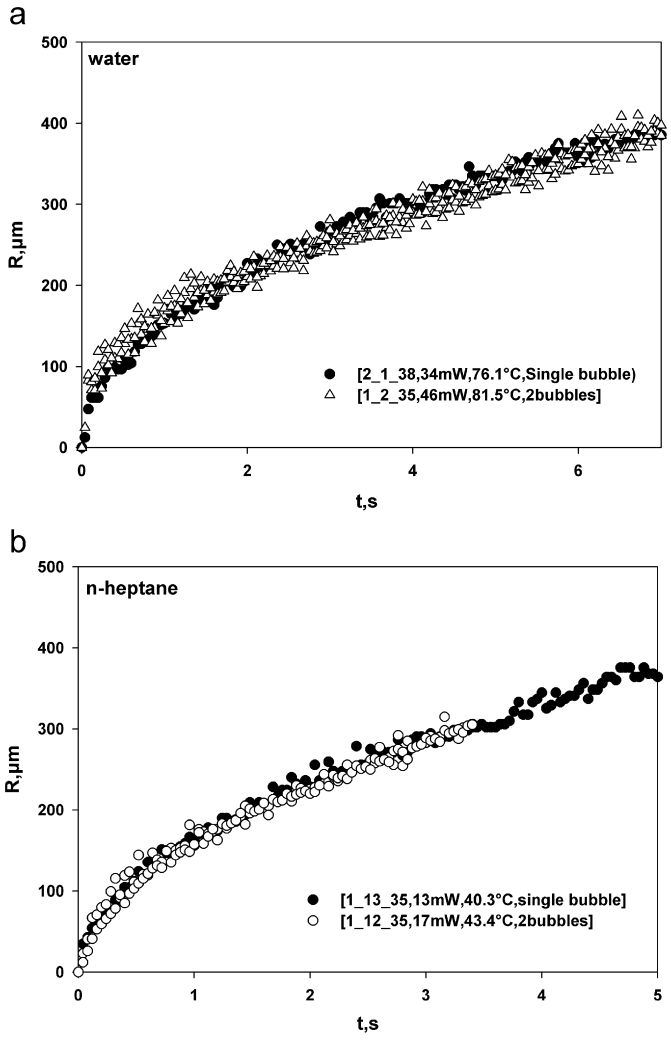

Fig. 6. Comparison of multiple with single bubble growth curves for (a) water (b) *n*-heptane.

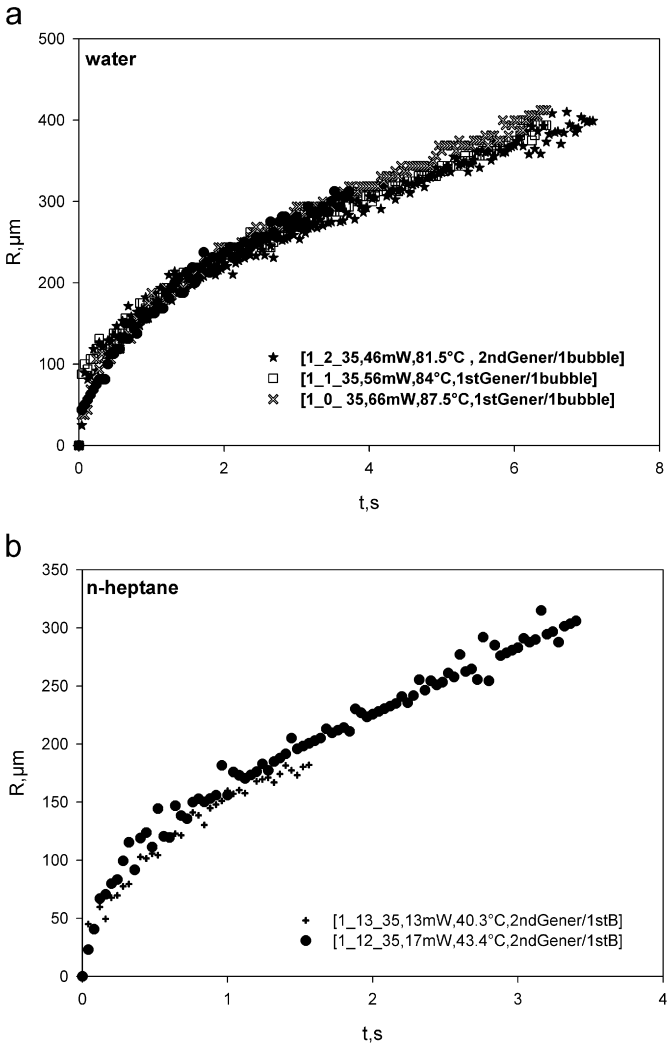

Fig. 7. Comparison of multiple bubble growth curves under different thermal conditions in order to determine the thermal saturation limit for (a) water (b) *n*-heptane.

small and their competition is not significant, the hotter two bubbles grow a bit faster than the respective single one.

Figs. 7a and b compares growth curves of double bubbles in water and *n*-heptane. Regardless of the different average thermistor temperatures among runs, the curves are comparable for both liquids. Divinis et al. (2004) working with single bubbles observed an upper temperature (saturation) limit above which any further increase in the thermistor temperature had practically no effect on bubble growth rate. This limit was found for water at $\sim 90\,^{\circ}C$ and for *n*-heptane at $\sim 55\,^{\circ}C$. It was argued that above these limits bubbles cannot grow any faster because their surface expands faster than the thermal boundary layer around the thermistor and so their growth is restricted by exposure to cold liquid layers. Figs. 7a and b indicate that saturation starts at lower temperatures for multiple bubbles than for single bubbles. This observation lends further support to the notion that adjacent bubbles may compete for the available dissolved carbon dioxide at the region of the heater. However, given the significance of this finding we feel that more work is needed to elucidate this issue.

4.5. Bubble nucleation

In water, the limited range of employed powers leads always to two active nucleation sites (Fig. 3). Bubbles growing during the first generation on the 1st site (preferred) nucleate without significant time delay. In particular, for a power of 46 mW the nucleation delay of the first bubble is 0.22 s whereas for 56 and 66 mW the delay is 0.09 s. Regarding the second bubble of the first generation (growing at the 2nd site), nucleation occurs after 2.84 s for the 46 mW run, but almost synchronously with the first bubble at higher powers.

The observed inversely proportional dependence of nucleation time delay on employed power (thermistor temperature) demonstrates that a nucleation energy barrier must be overcome for a site to become activated. It is believed that this effect is far more important than the reduction of contact angle of water with the thermistor at higher temperatures which also hampers heterogeneous nucleation (Wilt, 1986).

During later generations, the time that bubbles take to appear on the 1st site (after detachment of the previous bubbles) is between 0.12 and 0.28 s. The 2nd site needs an additional activation time (relative to the 1st site) between ~ 0.00 and 0.20 s. One might intuitively expect a rather immediate nucleation during the 2nd and 3rd bubble generations since nucleation cavities are already filled with gas left behind by departing bubbles (Kant and Weber, 1994; Liger-Belair et al., 2002). Nevertheless, nucleation time delay during later generations, may be seriously affected by the time needed for the concentration boundary layer of dissolved gas to be restored over

the heater following the detachment of a previous bubble (Jones et al., 1999b; Westerheide and Westwater, 1961).

In *n*-heptane, the above behavior is also confirmed (Fig. 4). For the 1st site, the nucleation delay is around 0.07 s for 13 mW, 0.03 s for 17 mW and ~ 0.00 s for 64 and 86 mW. The first activation of the 2nd site depends strongly on the delivered power. At a power of 13 mW the 2nd site is activated 6.48 s after nucleation at the 1st site, but this time delay drops to 2.84 s when the power is raised to 17 mW. Subsequent generations exhibit small (0.10–0.16 s) nucleation time delays at the lower power levels 13 and 17 mW and no discernable delay at the higher power levels 64 and 86 mW. Evidently, nucleation is more favorable in *n*-heptane than in water, a fact which is endorsed by the almost one order of magnitude higher solubility of carbon dioxide to *n*-heptane.

In addition, in *n*-heptane the number of active sites (at the same thermistor) increases drastically with increasing power level. Thus, when the power level is 13 and 17 mW there are two active sites but at 64 and 86 mW there exist five active sites. The dependence of the number of active sites on the delivered power supports further the notion of successively higher energy barriers needed to activate less favorable nucleation sites.

4.6. Bubble detachment

In the absence of buoyancy the main reason for bubble detachment is g-jitters. In experiments during the same parabolic flight campaigns (Divinis et al., 2004, 2006a) it was noticed that single bubbles in *n*-heptane were becoming floppy (sensitive to external vibrations) only when their radius was above 800 μm. Moreover, in water and in water/glycerin solutions bubbles were always stiff regardless their size because of the higher viscosity. So, at first glance, it seems peculiar that multiple bubbles in the present runs detach at a substantially smaller radius, between ~ 150 and ~ 450 μm (except the large coalescing bubble at very high powers in *n*-heptane; see below). Surprisingly, it is further noticed that the radius of detachment is comparable for *n*-heptane and water and independent of the applied power.

Inspection of Figs. 3 and 4 reveals a few more interesting features. Despite the appreciable lateral distance between simultaneous bubbles they always detach synchronously (within 40 ms, our image recording time resolution) regardless test liquid, power level and bubble size. Even during those 1st bubble generations that a substantial nucleation time delay exists between the two bubbles, the second, smaller, bubble detaches also synchronously with the first, larger, one. This is noteworthy because in previous single bubble experiments (Divinis et al., 2004, 2006a), whenever such a small bubble was left on the surface of the thermistor after the end of a heat pulse, it could not detach even during the high-gravity period (~ 1.8*g*) concluding a parabola. The above arguments combined suggest a clearly different detachment behavior of multiple bubbles compared to single bubbles.

Careful Inspection of the recorded frames shows a fundamental difference between the multiple bubble experiments in water and in *n*-heptane. In water, bubbles remain attached to their initial growth sites and depart synchronously (without coalescence) although they are apart by almost 180° around the thermistor's circumference (Fig. 8a). It is rather improbable that such simultaneous departure can be due to bubbles interaction through the intervening liquid layers. There is evidence that as a bubble grows its contact angle with the heater varies in a discontinuous manner, often with a stick-and-slip behavior (Buehl and Westwater, 1966). Apparently, small contact angles make detachment easy whereas large contact angles make detachment difficult. By employing high heat fluxes to create multiple bubbles the heater rapidly attains elevated temperatures although bubbles increase their size only gradually due to slow

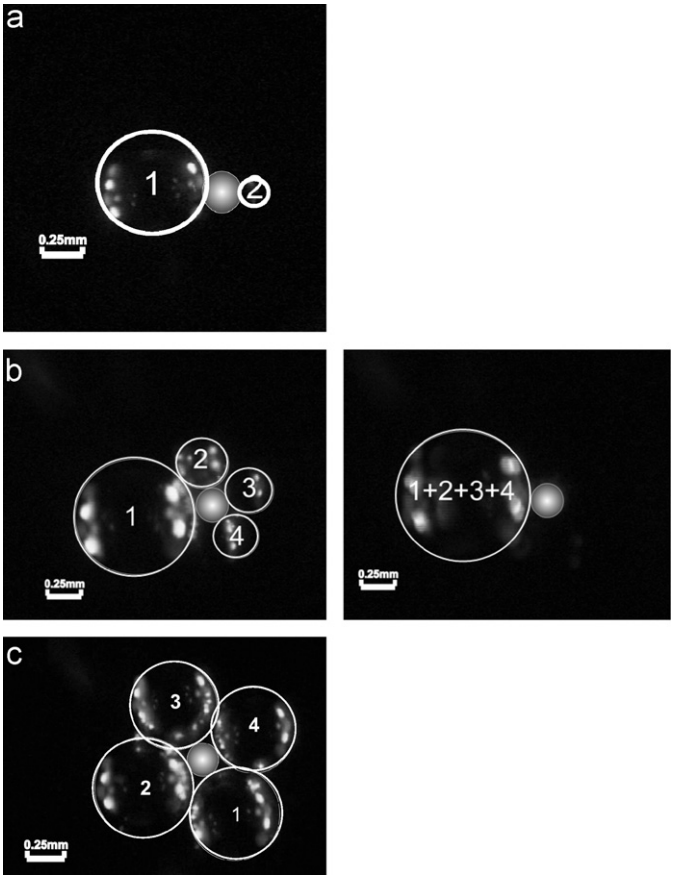

Fig. 8. Three characteristic moments of multiple bubble growth. (a) Two different size bubbles growing in water attached at their initial sites an instant before detachment. (b) Four different size bubbles growing in *n*-heptane before and after their coalescence. (c) Foam-like structure of four large bubbles growing simultaneously in *n*-heptane.

mass diffusion. Thus, at the elevated heater's temperature during multiple bubble growth the contact angle decreases and a serious destabilization of the contact line can be caused by g-jitters already at small bubble sizes.

Perhaps another explanation for the synchronous destabilization of the bubbles stems from the non perfect symmetry (sphericity) of the heater. These conditions may create appreciable temperature gradients along the contact line of the bubbles (contact angle gradients) causing lateral displacement and destabilization of the bubbles.

Contrary to water, in *n*-heptane, bubbles exhibit high mobility prior to departure. This is most likely due to the low capillary adhesion forces between the bubble and the heater as a result of the low values of surface tension and contact angle. Phenomena related to bubble mobility and induced interactions are described extensively by Divinis et al. (2006b). Here, we only note in relation to bubble departure that, at low power values (13 and 17 mW), bubbles of comparable size depart always after they have moved one towards the other and have coalesced while still in contact with the thermistor. In cases where a large and a small bubbles co-exist, the large one remains still and attracts the small one. In both cases, coalescence can create significant destabilizing forces.

At high powers (64 and 86 mW) three or more bubbles grow simultaneously during each generation (Figs. 8b and c). These bubbles soon become large enough and contact each other in a foam-like structure while they continue to grow. At some moment these bubbles coalesce into a new larger bubble which despite its excessive size continues to grow in contact with the heater during the subsequent generations. New bubbles appear around this large bubble

right after coalescence since the nucleation sites are now available. This is clearly seen in Figs. 4c (bubbles A and B, 3rd and 4th generations) and 4d (bubbles A–E, 2nd–6th generation). Such large bubbles are inherently unstable and should, in principle, detach easily. Recent studies (Wang et al., 2005; Lu and Peng, 2005) have demonstrated that when two bubbles grow next to each other they are attracted to the heater more strongly than when they are alone because the jet streams of the Marangoni flows around each bubble (pushing them away from the cold bulk and toward the heater) join together into a larger and more stable jet stream. This might be a plausible explanation for the unexpected stability of the large bubbles in Figs. 4c and d. Needless to say that this effect has a tremendous technological significance and adds to our understanding on the initiation of gas blanketing phenomena over solid walls in heat transfer equipment.

Also noteworthy in Fig. 4d is that bubble E (6th bubble generation) stops growing at 8.80 s because at that moment it is suddenly lifted-off from the surface of the thermistor by the other three bubbles that grow in contact with it. Bubble E does not drift away but stays in contact with the other three bubbles in a foam-like structure. This event has been presented in more detail by Divinis et al. (2006b) as it shows a serious potential for microgravity applications where heating surfaces need be periodically wiped from gas bubbles.

5. Conclusions

To generate multiple (two or more) simultaneous CO_2 bubbles in water and *n*-heptane—initially saturated with dissolved CO_2—higher power levels (heater temperatures) are needed compared with generating single bubbles. In addition, water requires higher powers than *n*-heptane chiefly because of its lower gas solubility. The number of simultaneous bubbles per generation and also the number of generations within a certain heating period increase with power level. This was best observed in *n*-heptane where multiple bubbles start to appear even at low power levels.

Simultaneous bubbles emerging at different sites of the heater do not grow at exactly the same rate whereas simultaneous bubbles of consecutive bubble generations growing at the same site usually do so. Using an appropriate theoretical model to estimate the average bubble temperature from the experimentally obtained bubble radius reveals that simultaneous bubbles do not grow isothermally to each other, apart from a short period at the beginning of heating when they are smaller than the size of the heater. This may be attributed to local deviations of the heater geometry from sphericity: bubbles with lower temperatures grow at higher-curvature regions. In addition, the temperature of both bubbles progressively diverges from the heater's temperature to an extent that varies between water and *n*-heptane. This behavior may be ascribed to the onset of Marangoni convection around the growing bubbles combined with the different speed of heat propagation in the two liquids.

Careful comparisons reveal that multiple bubbles grow at lower rates than single bubbles at equivalent thermal conditions, a fact which implies that multiple bubbles growing in proximity can deplete the dissolved gas in their neighborhood. The competition of adjacent bubbles for the available dissolved gas is further supported by the observed thermal saturation limit (temperature above which any increase in temperature has no effect on growth rate) for multiple bubbles which is distinctly lower than that for single bubbles.

Nucleation time delay and number of nucleation sites depend strongly on power level and liquid properties. Furthermore, multiple bubbles detach at some point along their growth due to g-jitters but this occurs through different paths for water and *n*-heptane. Nevertheless, in both liquids bubbles detach synchronously and at much smaller sizes than single bubbles do. This is attributed to the higher temperatures employed to produce multiple bubbles which are capable of destabilizing the contact line of the bubbles with the heater.

Acknowledgments

We are thankful to European Space Agency for kindly providing the parabolic flights (ESA MSN/GA/2003-51/JV). Also, the financial support by ESA through the project CBC (convective boiling and condensation: local analysis and modeling of dynamics and transfers, ESA-AO-2004-PCP-111/ELIPS-2) is gratefully acknowledged. We are particularly indebted to the many colleagues of the workshops in the Van der Waals–Zeeman Lab of the University of Amsterdam for the construction of the flight apparatus and to Dr. Robert de Bruijn for his contribution during the parabolic flight campaigns. This work is conducted under the umbrella of the COST P21 action: physics of droplets.

References

Barker, G.S., Jefferson, B., Judd, S.J., 2002. The control of bubble size in carbonated beverages. Chemical Engineering Science 57, 565–573.
Bisperink, C.G.J., Prins, A., 1994. Bubble growth in carbonated liquids. Colloids and Surfaces A: Physicochemical and Engineering Aspects 85, 237–253.
Buehl, W.M., Westwater, J.W., 1966. Bubble growth by dissolution: influence of contact angle. A.I.Ch.E. Journal 12, 571–576.
Chen, T., Chung, J.N., 2002. Coalescence of bubbles in nucleate boiling on microheaters. International Journal of Heat and Mass Transfer 45, 2329–2341.
Christopher, D.M., Wang, H., Peng, X.F., 2006. Numerical analysis of the dynamics of moving vapor bubbles. International Journal of Heat and Mass Transfer 49, 3626–3633.
Cooper, M.G., Judd, A.M., Pike, R.-A., 1978. Shape and departure of single bubbles growing at a wall. In: Proceedings of the 6th International Heat Transfer Conference, vol. II, pp. 115–120.
Divinis, N., Karapantsios, T.D., Kostoglou, M., Panoutsos, C.S., Bontozoglou, V., Michels, A.C., Sneep, M.C., de Bruijn, R., Lotz, H., 2004. Bubbles growing in supersaturated solutions at reduced gravity. A.I.Ch.E. Journal 50, 2369–2382.
Divinis, N., Kostoglou, M., Karapantsios, T.D., Bontozoglou, V., 2005. Self-similar growth of a gas bubble induced by localized heating: the effect of temperature-dependent transport properties. Chemical Engineering Science 60, 1673–1683.
Divinis, N., Karapantsios, T.D., de Bruijn, R., Kostoglou, M., Bontozoglou, V., Legros, J.C., 2006a. Bubble dynamics during degassing of dissolved gas saturated solutions at microgravity conditions. A.I.Ch.E. Journal 52, 3029–3040.
Divinis, N., Karapantsios, T.D., de Bruijn, R., Kostoglou, M., Bontozoglou, V., Legros, J.C., 2006b. Lateral motion and interaction of gas bubbles growing over spherical and plate heaters. Microgravity Science and Technology XVIII (3/4), 204–209.
Fogg, P.G.T., Gerrard, W., 1991. Solubility of gases in liquids: a critical evaluation of gas liquid systems in theory and practice. Wiley Interscience, New York.
Forster, H.K., Zuber, N., 1954. Growth of a vapor bubble in a superheated liquid. Journal of Applied Physics 25, 474–478.
Glas, J.P., Westwater, J.W., 1964. Measurements of the growth of electrolytic bubbles. International Journal of Heat and Mass Transfer 7, 1427–1443.
Harding, G.L., Window, B., 1982. Degassing of hydrogenated metal–carbon selective surfaces for evacuated collectors. Solar Energy Materials 7, 101–111.
Heide, K., Hartmann, E., Stelzner, Th., Müller, R., 1996. Degassing of a cordierite glass melt during nucleation and crystallization. Thermochimica Acta 280–281, 243–250.
Jones, S.F., Galvin, K.P., Evans, G.M., Jameson, G.J., 1998. Carbonated water: the physics of the cycle of bubble production. Chemical Engineering Science 53, 169–173.
Jones, F., Evans, G.M., Galvin, K.P., 1999a. Bubble nucleation from gas cavities—a review. Advances in Colloid and Interface Science 80, 27–50.
Jones, F., Evans, G.M., Galvin, K.P., 1999b. The cycle of bubble production from a gas cavity in a supersaturated solution. Advances in Colloid and Interface Science 80, 51–84.
Kant, K., Weber, M.E., 1994. Stability of nucleation sites in pool boiling. Experimental Thermal and Fluid Science 9, 456–465.
Kern, D.Q., 1950. Process Heat Transfer. McGraw-Hill, New York.
Kostoglou, M., Karapantsios, T.D., 2005. Approximate solution for a nonisothermal gas bubble growth over a spherical heating element. Industrial Engineering Chemistry Research 44, 8127–8135.
Kostoglou, M., Karapantsios, T.D., 2007. Bubble dynamics during the non-isothermal degassing of liquids. Exploiting microgravity conditions. Advances in Colloids and Surface Science (134–135), 125–137.
Lee, H.S., Merte Jr., H., Picker, G., Straub, J., 2003. Quasi-homogeneous boiling nucleation on a small spherical heater in microgravity. International Journal of Heat and Mass Transfer 46, 5087–5097.
Li, J., Peterson, G.P., 2005. Microscale heterogeneous boiling on smooth surfaces—from bubble nucleation to bubble dynamics. International Journal of Heat and Mass Transfer 48, 4316–4332.
Liger-Belair, G., Vignes-Adler, M., Voisin, C., Robillard, B., Jeandet, P., 2002. Kinetics of gas discharging in a glass of champagne: the role of nucleation sites. Langmuir 18, 1294–1301.

Liger-Belair, G., Voisin, C., Jeandet, P., 2005. Modeling nonclassical heterogeneous bubble nucleation from cellulose fibers: application to bubbling in carbonated beverages. Journal of Physical Chemistry B 109, 14573–14580.

Lu, J.F., Peng, X.F., 2005. Bubble separation and collision on thin wires during subcooled boiling. International Journal of Heat and Mass Transfer 48, 4726–4737.

Lubetkin, S.D., 1995. The fundamentals of bubble evolution. Chemical Society Reviews 24, 243–250.

Lubetkin, S.D., 1989a. The nucleation and detachment of bubbles. Journal of Chemical Society Faraday Transaction 1 85, 1753–1764.

Lubetkin, S.D., 1989b. Measurement of bubble nucleation rates by an acoustic method. Journal of Applied Electrochemistry 19, 668–676.

Malley, J.P., Edzwald, J.K., 1991. Concepts for dissolved-air flotation treatment of drinking waters. Water SRT-Aqua 40, 7–17.

McCabe, W.L., Smith, J.C., 1967. Unit Operations of Chemical Engineering. second ed. McGraw-Hill, New York.

Merte Jr., H., Lee, H.S., 1997. Quasi-homogeneous nucleation in microgravity at low heat flux: experiments and theory. Journal of Heat Transfer 119, 305–312.

Mori, B.K., 1998. Studies of bubble growth and departure from artificial nucleation sites. Ph.D. Thesis, Department of Mechanical and Industrial Engineering, University of Toronto.

Nyborg, L., Magalhuaes, S., 1996. Hot degassing of high alloy metal powders. Metal Powder Report 51, 38–53.

Payvar, P., 1987. Mass transfer controlled bubble growth during rapid decompression of a fluid. International Journal of Heat Mass Transfer 30, 699–706.

Perry, R.H., Chilton, C.H., 1973. Chemical Engineer's Handbook, fifth ed. McGraw-Hill, New York.

Petrovic, S., Robinson, T., Judd, R.L., 2004. Marangoni heat transfer in subcooled nucleate pool boiling. International Journal of Heat and Mass Transfer 47, 5115–5128.

Plesset, M.S., Zwick, S.A., 1954. The growth of vapor bubbles in superheated liquids. Journal of Applied Physics 25, 493–500.

Scriven, L.E., 1959. On the dynamics of phase growth. Chemical Engineering Science 10, 1–13.

Straub, J., Zell, M., Vogel, B., 1990. Pool boiling in a reduced gravity field. In: Hetsrony, (Ed.), Proceedings of the 9th International Heat Transfer Conference. Hemisphere, New York, pp. 129–155.

Straub, J., Zell, M., Vogel, B., 1992. Pool boiling under microgravity conditions. In: Proceedings of the First European Symposium Fluids in Space, Ajaccio, France, ESA SP-353.

Szekely, J., Fang, S.D., 1973. Non-equilibrium effects in the growth of spherical gas bubbles due to solute diffusion—II: the combined effects of viscosity liquid inertia, surface tension and surface kinetics. Chemical Engineering Science 28, 2127–2140.

Wang, H., Peng, X.F., Christopher, D.M., Lin, W.K., Pan, C., 2005. Investigation of bubble-top jet flow during sub-cooled boiling on wires. International Journal of Heat and Fluid Flow 26, 485–494.

Westerheide, D.E., Westwater, J.W., 1961. Isothermal growth of hydrogen bubbles during electrolysis. A.I.Ch.E. Journal 7, 357–362.

Wilt, P.M., 1986. Nucleation rates and bubble stability in water–carbon dioxide solutions. Journal of Colloid and Interface Science 112, 530–538.

Yamasaki, M., Iwamoto, K., Tamagawa, H., Kawamura, Y., Lee, J.K., Kim, H.J., Bae, J.C., 2007. Vacuum degassing behavior of Zr- Ni- and Cu-based metallic glass powders. Materials Science and Engineering A 449–451, 907–910.